Performance Analysis of GPS Carrier Phase Observable

WEIHUA ZHUANG, Member, IEEE
University of Waterloo

The accuracy analysis of Global Positioning System (GPS) carrier phase observable measured by a digital GPS receiver is presented. A digital phase-locked loop (DPLL) is modeled to extract the carrier phase of the received signal after a pseudorandom noise (PRN) code synchronization system despreads the received PRN coded signal. Based on phase noise characteristics of the input signal, the following performance of the first, second, and third-order DPLLs is analyzed mathematically: 1) loop stability and transient process; 2) steady-state probability density function (pdf), mean and variance of phase tracking error; 3) carrier phase acquisition performance; and 4) mean time to the first cycle-slipping. The theoretical analysis is verified by Monte Carlo computer simulations. The analysis of the dependency of the phase observable error on system dynamics, input noise and receiver design parameters provides with an important reference in designing the carrier phase synchronization system for high accuracy GPS positioning.

Manuscript received April 14, 1994; revised October 28, 1994.

IEEE Log No. T-AES/32/2/03456.

Author's address: Department of Electrical and Computer Engineering, University of Waterloo, Waterloo, Ontario, Canada N2L 3G1.

I. INTRODUCTION

The NAVSTAR (Navigation Satellite Timing and Ranging) Global Positioning System (GPS) is a satellite-based, worldwide, all-weather navigation and timing system. It is "the most significant development for safe and efficient navigation and surveillance of air and spacecraft since the introduction of radio navigation 50 years ago" [1]. The GPS is designed to provide precise position, velocity, and timing information on a global common grid system to an unlimited number of suitably equipped users. A GPS receiver is the key for a user to access the system. The major functions of the receiver are to provide a navigation processor with accurate pseudorange time delay, carrier beat phase, and Doppler frequency shift observables. Fundamentals and general function modeling of a digital GPS receiver have been presented in [2]. The pseudorange time delay observable can be obtained by a pseudorandom noise (PRN) code synchronizer [3]. The Doppler frequency shift observable can first be coarsely estimated in the PRN code synchronization, and then accurately tracked during the carrier phase synchronization. The carrier phase observable is a vital factor in achieving high GPS positioning accuracy [4]. However, the mathematical analysis of the carrier phase observable has not been studied in open literature. We present the modeling and performance analysis of the phase observable measured by a digital phase-locked loop (DPLL). It is expected that the analysis will help to improve the design of the DPLL, therefore, to reduce the phase observable error and to improve the GPS positioning accuracy.

DPLLs have been used to extract carrier phase [5]. Weinberg and Liu [6] first analyzed the first and second-order DPLLs with nonlinear phase detector in the presence of noise by numerically solving the Chapman-Kolmogorov (C-K) equation which describes the phase error process. Chie [7] extended the work to nth-order DPLLs. Analysis on DPLLs with a linear phase detector (digital tanlock loop) was presented by Lee and Un [8]. In the previous work, the C-K equation was applied to study the performance of DPLLs which tried to sample at the zero crossings of the input signal (i.e., nonuniform sampling). The phase of the incoming signal is measured against the reconstructed signal. Nyquist rate (NR)-DPLL is another type of DPLL, in which the input signal is sampled at the Nyquist rate (i.e., uniform sampling). The phase of the input signal is measured against a fix reference. The design of NR-DPLLs with a nonlinear phase discriminator was studied in [9, 10], however, the C-K equation was not used to study the probabilistic behaviors of the phase tracking error. Different from the previous work, this paper has the following two unique aspects in DPLL performance analysis. 1) DPLLs with a linear phase

discriminator and uniform sampling are studied. The linear phase discriminator provides wider lock range, less steady-state phase error, and improved stability; and uniform sampling of the received GPS signal can achieve simplicity and flexibility in the receiver design. The C-K equation is applied to investigate the probabilistic performance of phase tracking errors and other characteristics of the loops, such as phase acquisition probability, and mean time to the first cycle slip. 2) The DPLL is inter-connected with the PRN code synchronizer since GPS system uses spread spectrum signaling waveforms and the effect of PRN code synchronization on carrier phase tracking is considered. Because of very low signal-to-noise ratio (SNR) of the input signal, the DPLL can only operate on the code-free signal after the DDLL succeeds in tracking and despreading the input PRN code. The special input signal and noise characteristics result in the necessity of further loop performance analysis. Based on phase noise characteristics of the input signal, the following performance of the first, second, and third-order DPLLs is analyzed mathematically: 1) loop stability and transient process; 2) steady-state probability density function (pdf), mean and variance of phase tracking error; 3) carrier phase acquisition performance; and 4) mean time to the first cycle-slipping. The effects of DPLL structures and parameters on the GPS carrier phase observable error are analyzed mathematically. The analysis gives an accurate description of error sources of the observable and how the sources degrade the observable accuracy.

This work is organized as follows. Section II presents the DPLL modeling for a GPS receiver, the analysis of the loop input signal, and carrier phase noise characteristics. In the absence of the input noise, the DPLL stable region and phase tracking transient process are analyzed in Section III. The steady-state pdf, mean and variance of phase error in the presence of input noise are derived in Section IV. Section V studies the performance of phase acquisition and mean time to the first cycle-slipping. The first, second, and third-order DPLLs are considered in the analysis. Section VI demonstrates computer simulation results which verify the theoretical analysis, followed by the conclusions in Section VII.

II. SYSTEM MODELING

Fig. 1 is a simplified functional block diagram of the digital baseband processor (DBP) of the GPS receiver, which performs the maximum-likelihood estimation of the GPS observables. The pseudorange time delay is measured by accurately tracking the PRN code phase of the input GPS signal using a digital energy detector and a digital early-late (E-L) delay lock loop (DDLL). The receiver generates an identical PRN code signal to synchronize the PRN code of the input signal from a GPS satellite. The digital

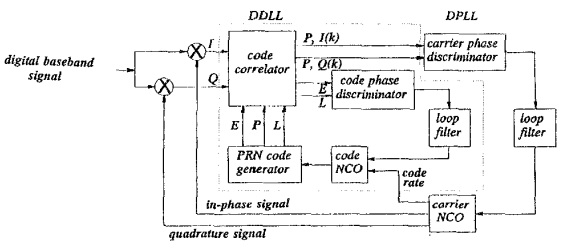

Fig. 1. Functional block diagram of DBP.

energy detector sweeps the uncertainty ranges of the input code phase and Doppler frequency shift with discrete steps, and senses the coarse synchronization (acquisition) of the PRN code phase and Doppler shift between the input and local signals. The DDLL accurately tracks the variations of the incoming code phase and keeps the code phase alignment error within an allowable limit after the code phase acquisition. From the accurate tracking of the input PRN code phase, the pseudorange time delay can be obtained and the input signal can be despreaded. A "prompt" (P) channel is set for carrier phase tracking. The despread inphase (I) and quadrature (Q) components of the received signal at baseband pass to the DPLL for carrier phase synchronization. From the carrier phase tracking, both integer and fractional cycles of carrier beat phase of the signal derived from differencing (beating) the incoming Doppler-shifted carrier with a local signal of no Doppler shift, and the Doppler shift of the received carrier signal can be estimated accurately. Coherent correlation for tracking code phase and carrier phase is then initiated. Code synchronization and despreading are performed prior to carrier phase tracking since sufficient SNR is necessary for the DPLL to operate successfully (to be discussed). After the PRN code is removed, the signal SNR is increased by the despreading gain. The major components of a DPLL are a carrier phase discriminator, a loop filter and a numerically controlled oscillator (NCO). The phase and frequency of the NCO are numerically controllable. Therefore, under the condition that the phase tracking residual of the DPLL is negligible, the output of the local NCO can be used to remove the carrier component of the input signal and, at the same time, the phase and Doppler frequency shift of the incoming signal can be obtained from those of the local NCO (after being modified with the carrier phase residual) [2].

A. Loop Difference Equations

As shown in Fig. 1, the phase discriminator works on the outputs of the in-phase and quadrature correlators at a rate (f_s/N) after the DDLL despreads the PRN code of the input signal, where f_s is the sampling rate and N is the number of data samples in each DDLL correlation interval. A functional diagram

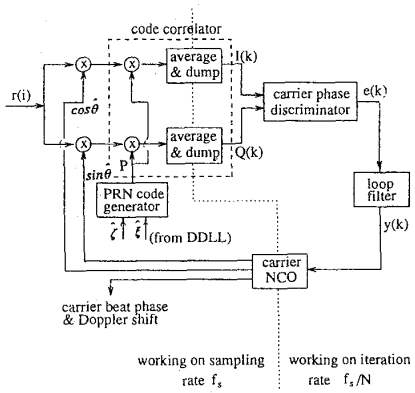

Fig. 2. Block diagram of DPLL.

of the DPLL is shown in Fig. 2, where only the prompt (P) PRN code is shown to remove the input PRN code for carrier synchronization. The NCO generates the local in-phase and quadrature reference signals at the sampling rate f_s for noncoherently correlating (in the carrier phase acquisition process) or coherently correlating (in the carrier phase fine tracking process) the input signal. The output of the loop filter modifies the phase and frequency of the NCO every NT_s. The ith sample GPS received signal at baseband is

$$r(i) = AP[(1+\zeta)iT_s - \xi T_p]\cos[(\omega_b + \omega_d)i + \phi_0] + n(i) \tag{1}$$

where $P[\cdot]$ is a ± 1-valued PRN code with rate R, delayed by $\tau = \xi T_p$ with respect to the GPS system time (T_p is the code chip width), ω_b $(= 2\pi f_b T_s)$ and ω_d $(= 2\pi f_d T_s)$ are the digital radian frequencies corresponding to the baseband carrier frequency f_b and Doppler shift f_d (T_s is the sampling period), ϕ_0 is the initial carrier phase at $i = 0$, and $n(i)$ is the equivalent input Gaussian noise at baseband. Because of the two-fold impact of the Doppler shift on the received signal (i.e., carrier frequency offset and code rate offset), the code rate R is equal to $(1+\zeta)R_0$, where $\zeta = f_d/f_L$ (f_L is the RF frequency), and R_0 is the code rate without the Doppler shift. The A/D converter in front of the DBP can be designed to provide high immunity to non-Gaussian interference and jamming, therefore, it is reasonable to assume that the input noise at baseband is Gaussian band-limited white noise, with the bandwidth determined by the lowpass filter preceding the A/D converter. With the local PRN code signal $P[(1+\hat{\zeta})iT_s - \hat{\xi}T_p]$ and the local inphase and quadrature signals in the kth correlation interval $\cos[(\omega_b + \hat{\omega}_{dk})i + \hat{\phi}_{k-1}]$ and $\sin[(\omega_b + \hat{\omega}_{dk})i + \hat{\phi}_{k-1}]$ $(i = 0,1,\ldots,N-1)$ respectively (where $\hat{x}$ represents the estimate of x), following the procedure similar to that of deriving [3, (8)–(9)], the signal $I(k)$ and $Q(k)$ from the in-phase and quadrature channel correlators (Fig. 2) at the end of the kth correlation interval are

$$\begin{aligned} I(k) &= \frac{A}{2}R(\tau - \hat{\tau})\text{sinc}[(\Delta\omega_d)_k N/2] \\ &\quad \times \cos[\theta(k) - \hat{\theta}(k)] + N_I(k) \\ Q(k) &= \frac{A}{2}R(\tau - \hat{\tau})\text{sinc}[(\Delta\omega_d)_k N/2] \\ &\quad \times \sin[\theta(k) - \hat{\theta}(k)] + N_Q(k) \end{aligned} \tag{2}$$

where $(\Delta\omega_d)_k = \omega_{dk} - \hat{\omega}_{dk}$ is the Doppler shift estimation error in the kth interval, $\theta(k)$ and $\hat{\theta}(k)$ are the phases of the incoming signal and the local NCO signal at the center of the interval, $N_I(k)$ and $N_Q(k)$ are the lumped noise components of $I(k)$ and $Q(k)$, respectively. The linear phase discriminator performs an arc-tangent operation, which has an output

$$\begin{aligned} &e(k) = \arctan[Q(k)/I(k)] = g[\psi(k)] + n_\theta, \\ &e(k) \in [-\pi, +\pi] \end{aligned} \tag{3}$$

where $g[\cdot]$ is the characteristic function of the phase discriminator, $\psi(k) = \theta(k) - \hat{\theta}(k)$ is the phase tracking error due to a noise-free incoming signal and $n_\theta(k) \in (-\pi - g[\psi(k)], +\pi - g[\psi(k)])$ is the phase disturbance due to the input noise. Since the values of $I(k)$ and $Q(k)$ are known, there is no ambiguity in distinguishing the phase error in the domain $[-\pi, +\pi]$. In the absence of the noise, $e(k)$ is equal, in the modulo $[-\pi, +\pi]$ sense, to the phase error between the incoming signal and the local NCO signal at the center of the kth correlation interval. As a result, the characteristic curve of the phase discriminator is linear with period 2π,

$$g[\psi(k)] = \psi(k) \text{mod}[-\pi, +\pi]. \tag{4}$$

The linear characteristics due to using $\arctan[\cdot]$ operation is unique and has many advantages over the nonlinear characteristics of the $\arcsin[\cdot]$ operation [8, 11–12]. A mathematically equivalent model of the DPLL is shown in Fig. 3. With the NCO transfer function $D(z) = z^{-1}/(1-z^{-1})$ and loop filter transfer function $F(z)$ (where z^{-1} is the unit delay operator $z^{-1}\{x(k)\} = x(k-1)$), the corresponding loop equations are

$$\begin{aligned} \psi(k) &= \theta(k) - \hat{\theta}(k) \\ e(k) &= g[\psi(k)] + n_\theta(k) \\ y(k) &= F(z)e(k) \\ \hat{\theta}(k) &= D(z)y(k) = \sum_{i=0}^{k-1} y(i) \end{aligned} \tag{5}$$

where $y(k)$ is the output of the loop filter at the end of the kth correlation interval.

B. Characteristics of Phase Noise $n_\theta(k)$

It has been shown [13] that $N_I(k)$ ad $N_Q(k)$ in (2) are Gaussian if $N \gg 1$, with expectations $E[N_I(k)] =$

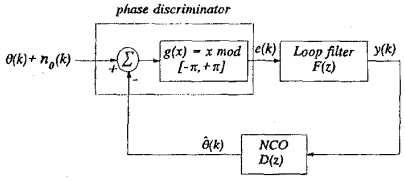

Fig. 3. Mathematical modeling of DPLL.

0, $E[N_Q(k)] = 0$, and variances $\text{var}[N_I(k)] = \text{var}[N_Q(k)] \approx \sigma_n^2/2N$, respectively (where σ_n^2 is the variance of the input noise component $n(i)$); furthermore, $N_I(k)$ and $N_Q(k)$ are uncorrelated. As a result, $I(k)$ and $Q(k)$ are also mutually independent Gaussian random variables with the means and variances given as follows

$$\begin{aligned} E[I(k)] &= D_k \cos\psi(k), \\ E[Q(k)] &= D_k \sin\psi(k) \\ \text{var}[I(k)] &= \text{var}[Q(k)] = \text{var}[N_I(k)] \\ &= \text{var}[N_Q(k)] \approx \sigma_n^2/2N \triangleq \sigma^2 \end{aligned} \tag{6}$$

where $D_k = (A/2) \cdot R(\tau - \hat{\tau}) \cdot \text{sinc}[(\Delta\omega_d)_k N/2]$ and $R(\cdot)$ is the auto-correlation function of the PRN code. Accordingly, the joint pdf of the amplitude $C(k) \triangleq \{I^2(k) + Q^2(k)\}^{0.5}$ and the phase discriminator output $e(k)$ is

$$\begin{aligned} &p(C(k), e(k)) \\ &= \frac{C(k)}{2\pi\sigma^2} \exp\left\{ -\frac{1}{2\sigma^2}[C^2(k) + D_k^2 - 2C(k)D_k \right. \\ &\qquad \left. \times \cos(e(k) - \psi(k))] \right\} \end{aligned} \tag{7}$$

for $C(k) \geq 0$, and $p(C(k), e(k)) = 0$ for $C(k) < 0$. Integrating (7) with respect to $C(k)$ from 0 to ∞, we obtain the pdf of phase error

$$\begin{aligned} p(e(k)) &= \frac{1}{2\pi} \exp(-\alpha) + \frac{\sqrt{2\alpha}}{2\pi} \cos(e(k) - \psi(k)) \\ &\quad \times \exp[-\alpha \sin^2(e(k) - \psi(k))] \\ &\quad \times \int_{-\infty}^{\sqrt{2\alpha}\cos(e(k)-\psi(k))} \exp\left(-\frac{u^2}{2}\right) du \end{aligned} \tag{8}$$

where

$$\alpha \triangleq D_k^2/2\sigma^2 = \tfrac{1}{2} \cdot \alpha_i \cdot N \cdot R^2(\tau - \hat{\tau}) \cdot \text{sinc}^2[(\Delta\omega_d)_k N/2] \tag{9}$$

represents the actual SNR value of the input signal of the phase discriminator, with $\alpha_i \triangleq A^2/2\sigma_n^2$ being the SNR value of the received signal at baseband. By (6), the actual SNR value is increased by the correlation interval N and is decreased by $R^2(\tau - \hat{\tau})$ due to the DDLL tracking error $(\tau - \hat{\tau})$ and by $\text{sinc}^2[(\Delta\omega_d)_k N/2]$ due to the Doppler frequency shift tracking error $(\Delta\omega_d)_k$. The increase of N is limited if $(\Delta\omega_d)_k \neq 0$. As a result, in order to achieve sufficiently high SNR for the DPLL to accurately track the input carrier phase and frequency, the DDLL should keep accurate synchronization with the input PRN code, i.e., $|\tau - \hat{\tau}| \to 0$, so that $R(\tau - \hat{\tau}) \to 1$. This confirms that the carrier phase tracking can be performed only after the input PRN code phase has been accurately synchronized. It is also noticed that, although $e(k)$ ranges only from $-\pi$ to $+\pi$ because of the Mod$[-\pi, +\pi]$ operation in the arctan$[\cdot]$ function, $P(e(k))$ itself is periodic in $e(k)$ with period 2π and has peaks occurring at $e(k) = g[\psi(k)] + 2l\pi$ for all integer values of l. With $e(k) \in (-\pi, +\pi)$, $p(e(k))$ reaches its maximum value at $e(k) = g[\psi(k)]$ which is the phase tracking error in the absence of the incoming noise. Decomposing $e(k)$ into $g[\psi(k)]$ (noise-free tracking error) and $n_\theta(k)$ (due to the incoming noise) as shown in (3) and letting $|\psi(k)| < \pi$ (i.e., ignoring the integer cycles of phase error), we have

$$\begin{aligned} &n_\theta(k) = e(k) - \psi(k) \\ &n_\theta(k) \in (-\pi - g[\psi(k)], +\pi - g[\psi(k)]). \end{aligned} \tag{10}$$

From (8) and using the fact that $n_\theta(k)$ are mutually independent for different k because of the "Average & Dump" operation in the correlators, the pdf of the random phase noise component $n_\theta(k)$ is

$$\begin{aligned} p(n_\theta(k)) &= \frac{1}{2\pi} \exp(-\alpha) + \frac{\sqrt{\alpha}\cos n_\theta(k)}{\sqrt{\pi}} \\ &\quad \times \exp[-\alpha \sin^2 n_\theta(k)] \\ &\quad \times \{\tfrac{1}{2} + \text{erf}[\sqrt{2\alpha}\cos n_\theta(k)]\} \end{aligned} \tag{11}$$

where erf$(\cdot)$ is the standard Gaussian distribution function. Based on (11), if α is large enough so that the first component of the pdf is much smaller than the second component, the pdf $p(n_\theta(k))$ has its peak at $n_\theta(k) = 0$, resulting from the fact that $p(e(k))$ has its peak value at $e(k) = \psi(k)$ (corresponding to noise-free tracking error); otherwise, if α is very small, the noise component $n_\theta(k)$ dominates the output of the phase discriminator, and the noise is almost uniformly distributed from $-\pi$ to $+\pi$ irrespective of the value of $\psi(k)$, in which case accurate phase tracking becomes impossible.

From the above discussion, the output of the phase discriminator consists of both error $g[\psi(k)]$ due to incoming signal phase dynamics and error $n_\theta(k)$ due to incoming additive noise. In the following, we analyze the error component resulting from system dynamics in Section III and from noise in Section IV.

III. LOOP STABILITY AND TRANSIENT PROCESS

In the absence of input noise, the random phase noise $n_\theta(k)$ vanishes so that $e(k) = g[\psi(k)] = [\theta(k) - \hat{\theta}(k)] \bmod [-\pi, +\pi]$. The phase tracking error is called the restricted phase error process and is represented by $\Psi(k)$. In carrier phase fine tracking, $|\theta(k) - \hat{\theta}(k)| < \pi$, the loop (5) can be represented on z-plane as

$$\psi(z) = \frac{\theta(z)}{1 + F(z)D(z)} \tag{12}$$

which gives the dependency of phase tracking error $\psi(z)$ on input phase $\theta(z)$ and loop filter $F(z)$. The loop locking condition and phase tracking error (due to input phase dynamics) of first, second, and third-order loops can be analyzed based on (12).

The First-Order Loop: The transfer function of the loop filter is $F(z) = G_1$, therefore, the loop equation is

$$\psi(k) - (1 - G_1)\psi(k-1) = \theta(k) - \theta(k-1). \tag{13}$$

With a linear input carrier phase $\theta(k) = a_1 k + a_0$, $k \geq 0$, $\psi(k)$ converges to a steady-state tracking error $\psi_{ss} = a_1/G_1$, independently of the initial phase error if $|1 - G_1| < 1$ and if $|\psi(k)| < \pi$. The strictest restriction corresponding to the latter condition is: when $\psi(k-1) = \pm\pi$, $|\psi(k)|$ must be less than π. As a result, the loop locking condition is

$$\begin{aligned} &|a_1/\pi| < G_1 < 2 - |a_1/\pi| \\ &|a_1/\pi| < 1. \end{aligned} \tag{14}$$

If the dynamics parameter $|a_1|$ (representing frequency) of the input phase increases, the possible range of G_1 decreases for a stable loop. The transient responses are plotted in Fig. 4 for different G_1 values with initial phase tracking error $\psi(0) = 1$ (rad) and input phase $\theta(k) = 0.1k + 0.5$. It is shown that the steady-state phase tracking error decreases as the loop gain G_1 increases, and the fast convergence is achieved with $G_1 = 1.0$. The lock-in frequency $\Delta\omega_L$ of the DPLL is defined as the maximum initial frequency offset to achieve synchronization without cycle-slipping under the worst initial phase conditions [14]. From (14), it is required that $|a_1| < \pi$ for the loop to lock to the input phase without cycle-slipping. Taking the correlation interval $T = NT_s$ into account, the lock-in frequency is $|\Delta\omega_L| = |a_1|/T < \pi/(NT_s)$. Reducing the correlation interval (NT_s) increases the loop lock-in frequency $|\Delta\omega_L|$.

The Second-Order Loop: The transfer function of the loop filter is $F(z) = G_1 + G_2/(1 - z^{-1})$, where G_1 and G_2 are loop gain parameters. Substituting $F(z)$ into (12), we obtain the loop equation

$$\begin{aligned} &\psi(k) - 2\psi(k-1) + \psi(k-2) \\ &\quad = [\theta(k) - 2\theta(k-1) + \theta(k-2)] \\ &\qquad - (G_1 + G_2)\psi(k-1) + G_1\psi(k-2). \end{aligned} \tag{15}$$

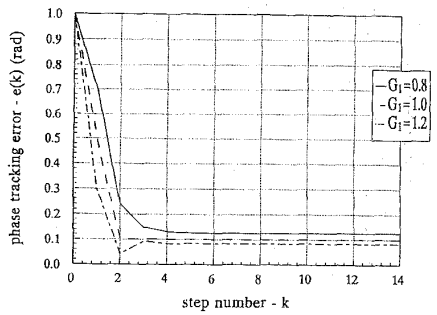

Fig. 4. First-order DPLL transient processes: $\theta(k) = 0.1k + 0.5$ (rad), $e(0) = 1.0$ (rad).

With a quadratic phase input $\theta(k) = a_2k^2 + a_1k + a_0$, $k \geq 0$, for the loop to be stable requires

$$\begin{aligned} &r \triangleq 1 + G_2/G_1 > 1 \\ &0 < G_1 < \frac{4}{1+r}. \end{aligned} \tag{16}$$

In addition, it is necessary that $|\psi(k)| < \pi$ even when $|\psi(k-1)| = |\psi(k-2)| = \pm\pi$. In view of these properties, the following two conditions must be satisfied. First, when $\psi(k-2) = \pi$ and $\psi(k-1) = \pm\pi$, $\psi(k)$ must be inside region $(-\pi, +\pi)$, which results in

$$2 - \left|\frac{2a_2}{\pi}\right| < G_1(r+1) < 4 - \left|\frac{2a_2}{\pi}\right|. \tag{17}$$

Secondly, when $\psi(k-2) = -\pi$ and $\psi(k-1) = \pm\pi$, $\psi(k)$ must be inside region $(-\pi, +\pi)$, which results in

$$\left|\frac{2a_2}{\pi}\right| < G_1(r-1) < 2 - \left|\frac{2a_2}{\pi}\right|. \tag{18}$$

In summary, the overall loop locking condition can be derived as

$$\begin{aligned} &2 + \frac{2|a_2|}{\pi} < G_1(r+1) < 4 - \frac{2|a_2|}{\pi} \\ &\frac{2|a_2|}{\pi} < G_1(r-1) < 2 - \frac{2|a_2|}{\pi} \\ &r > 1 \\ &|a_2| < \frac{\pi}{2}. \end{aligned} \tag{19}$$

Two examples of the stable region on the loop gain parameter $G_1 - r$ plane are plotted in Fig. 5, with the system dynamic parameter 1) $|a_2| = 0$ and 2) $|a_2| = \pi/4$. It is seen that the stable region is a function of input phase dynamics; with $|a_2|$ increased from 0 to $\pi/4$, the stable region is greatly reduced. The transient responses are plotted in Fig. 6 for different r values with initial tracking error $\psi(-1) = 0.0$, $\psi(0) = 1$ (rad), $G_1 = 1.0$, given the input phase $\theta(k) = 0.125k^2 + 0.5k + 1.0$. It is observed that the increase of loop parameter r reduces the steady-state phase tracking error; however, for each G_1 value in the stable region,

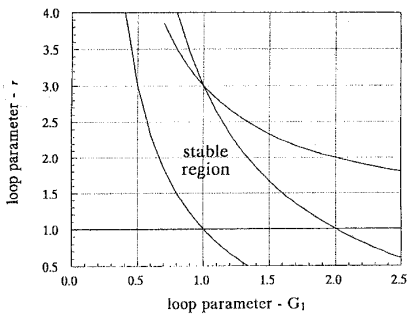

(a)

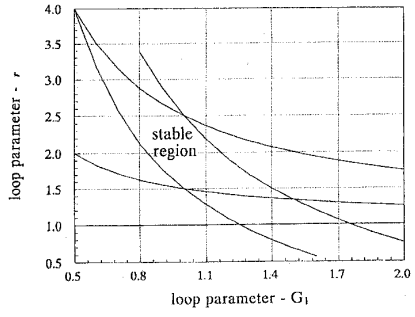

(b)

Fig. 5. Second-order DPLL stable regions. (a) $|a_2| = 0$. (b) $|a_2| = \pi/4$.

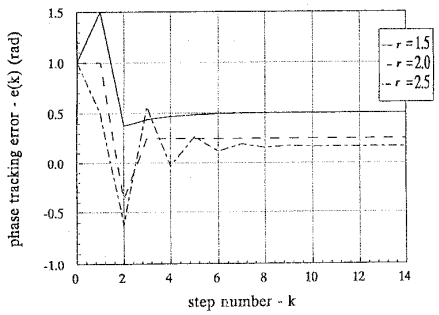

Fig. 6. Second-order DPLL transient processes: $\theta(k) = 0.125k^2 + 0.5k + 1.0$ (rad), $G_1 = 1.0$, $\psi(-1) = 0.0$, $\psi(0) = 1.0$ (rad).

the selection of r is limited corresponding to each $|a_2|$ value (as shown in Fig. 5). The fast convergence is achieved with $r = 2.0$. The second-order loop can acquire the input phase of any frequency a_1, therefore, it has very wide lock-in frequency range which is only limited by $f_s/2N$ (i.e., half of the rate which the NCO updates its phase and frequency).

The Third-Order Loop: The transfer function of the loop filter is $F(z) = G_1 + G_2/(1 - z^{-1}) + G_3/(1 - z^{-1})^2$, where G_1, G_2, and G_3 are loop gain parameters. With a cubic phase input $\theta(k) = a_3k^3 + a_2k^2 + a_1k + a_0$, $k \geq 0$, and letting $p \triangleq 1 + G_2/G_1 + G_3/G_1$, the loop stability conditions are

$$\begin{aligned} P - R &> 0 \\ P + R - 2 &> 0 \\ (P-1)G_1 - P + R &> 0 \\ 8 - (P + R + 2)G_1 &> 0. \end{aligned} \tag{20}$$

It is also required that $|\psi(k)| < \pi$ when $|\psi(k-3)| = |\psi(k-2)| = |\psi(k-1)| = \pi$. Similar to the analysis (17)–(18) of a second-order loop, the overall loop stable conditions independent of the initial phase tracking error can be further derived as

$$\begin{aligned} \frac{6|a_3|}{\pi} - 2 < (r-p)G_1 &< -\frac{6|a_3|}{\pi} \\ 4 + \frac{6|a_3|}{\pi} < (p+r)G_1 &< 6 - \frac{6|a_3|}{\pi} \\ 6 + \frac{6|a_3|}{\pi} < (p+r+2)G_1 &< 8 - \frac{6|a_3|}{\pi} \\ \frac{6|a_3|}{\pi} < (2+r-p)G_1 &< 2 - \frac{6|a_3|}{\pi}. \end{aligned} \tag{21}$$

The last condition in (21) requires that $a_3 < \pi/6$; otherwise loop stability is impossible if $|\psi(k-3)| = |\psi(k-2)| = |\psi(k-1)| = \pi$. Hence, the loop can track a cubic input phase with dynamic $|a_3|$ up to $\pi/6$. According to (21), the stable region on the $r - p$ plane of loop parameters is shown in Fig. 7 with $G_1 = 1.0$ and 1) $|a_3| = 0.0$, and 2) $|a_3| = \pi/12$. The increase of input phase dynamics shrinks the stable region on the $r - p$ plane given a G_1 value. Larger r and p values are required in order for the loop to track an input phase $\theta(k)$ with higher dynamics. Fig. 8 shows the loop transient responses with initial phase error $\psi(0) = 1.0$ (rad), $G_1 = 1.0$, $r = 2.0$ and several values of p, given that $\theta(k) = (0.125/6)k^3 + 0.25k^2 + 0.5k + 1.0$ (rad). It is noticed that the increase of the loop gain parameter p reduces the steady-state phase error, and the fast convergence is achieved with $G_1 = 1.0$, $r = 2.0$ and $p = 3.0$. However, the largest p value is limited as seen from Fig. 7. As in the case of the second-order loop, the third-order loop can acquire the input phase of any frequency a_1, hence it has a very wide lock-in frequency range which is limited only by $f_s/2N$.

Based on the above noise-free performance analysis, it is observed that higher order loops have better dynamic tracking performance (which means smaller tracking error and faster convergence) and lower order loops are more stable. Hence higher order loops achieve better dynamic tracking capability by sacrificing loop stability. Both dynamic capability and stability of the loops must be taken into account in the DPLL design. In lower system dynamic environments, lower order of loops are better due to their stability. However in higher system dynamic environments, higher order loops with larger gain parameters

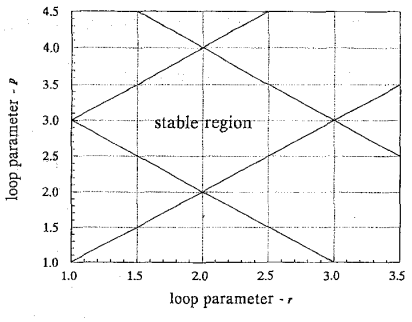

(a)

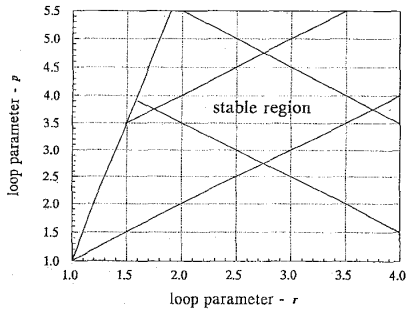

(b)

Fig. 7. Third-order DPLL stable regions. (a) $|a_3| = 0$, $G_1 = 1.0$. (b) $|a_3| = \pi/12$, $G_1 = 1.0$.

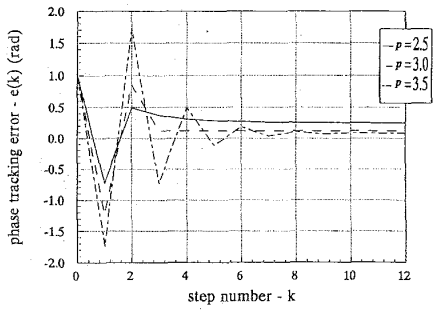

Fig. 8. Third-order DPLL transient processes: $G_1 = 1.0$, $r = 2.0$, $\psi(-2) = \psi(-1) = 0.0$, $\psi(0) = 1.0$ (rad), $\theta(k) = (0.125/6.0)k^3 + 0.25k^2 + 0.5k + 1.0$ (rad).

are preferred because of their improved dynamic performance.

IV. THE PDF AND VARIANCE OF PHASE TRACKING ERROR

Due to the stochastic nature of the input phase noise, the phase tracking error is also a stochastic process. In this section, we apply the C-K equation to study the pdf, mean and variance of the phase error. The pdf of phase tracking error gives a complete probabilistic picture of how the input noise affects phase tracking accuracy. On the other hand, we may wish to use a single number, such as the variance of phase error, to describe the DPLL capability of suppressing noise effects. In the following, we derive the mathematical expressions of the pdf and variance of phase error due to the input noise. Accurate description of how the phase error depends on the loop parameters and input noise statistics is presented.

The First-Order Loop: For the linear input phase, the loop equation of the unrestricted phase error process $\{\psi(k)\}$ is, from (5),

$$\psi(k) = \psi(k-1) - G_1 g[\psi(k-1)] - G_1 n_\theta(k-1) + a_1. \tag{22}$$

Since the phase noise components $n_\theta(k)$ are mutually independent for different k, the phase tracking error process $\{\psi(k)\}$ is a first-order, discrete time, continuously variable Markov process [15]. Given an initial phase error $\psi_0 \triangleq \psi(0)$, the pdf of $\psi(k)$ satisfies the following C-K equation

$$p_k(\psi \mid \psi_0) = \int_{-\infty}^{\infty} q_{k-1}(\psi \mid u) p_{k-1}(u \mid \psi_0)\, du \tag{23}$$

where $q_{k-1}(\psi \mid u)$ is the conditional pdf of $\psi(k)$ given $\psi(k-1) = u$. Because $n_\theta(k) \in (-\pi - g[\psi(k)], +\pi - g[\psi(k)])$, from (3), ψ of $q_{k-1}(\psi \mid u)$ ranges from $(u + a_1 - G_1\pi)$ to $(u + a_1 + G_1\pi)$. And from (11), $q_{k-1}(\psi \mid u)$ can be derived as

$$q_{k-1}(\psi \mid u) = \begin{cases} \dfrac{1}{G_1}\dfrac{\exp(-\alpha)}{2\pi} + \dfrac{1}{G_1}\dfrac{\sqrt{\alpha}}{\sqrt{\pi}}\cos\left(\dfrac{\psi - \psi_p}{G_1}\right) \\ \quad \times \exp\left[-\alpha \sin^2\left(\dfrac{\psi - \psi_p}{G_1}\right)\right] \\ \quad \times \left\{\dfrac{1}{2} + \operatorname{erf}\left[\sqrt{(2\alpha)}\cos\left(\dfrac{\psi - \psi_p}{G_1}\right)\right]\right\} \\ \quad \text{if} \quad \psi \in (u + a_1 - G_1\pi, u + a_1 + G_1\pi) \\ 0, \quad \text{if} \quad \psi \notin (u + a_1 - G_1\pi, u + a_1 + G_1\pi) \end{cases} \tag{24}$$

where $\psi_p = u + a_1 - G_1 \cdot g[u]$. In the above equation, ψ is defined only in the interval $(u + a_1 - G_1\pi, u + a_1 + G_1\pi)$ although ψ and u are defined in the interval $(-\infty, +\infty)$ in (23). Usually the pdf of the phase tracking error in the domain $(-\pi, +\pi)$ is of interest. We introduce periodicity into the conditional pdf of the phase tracking error (which is independent of k) as

$$r(\Psi \mid u) \triangleq \sum_{n=-\infty}^{\infty} q_{k-1}(\Psi + 2n\pi \mid u) \tag{25}$$

where $\Psi(k) \triangleq g[\psi(k)] \in (-\pi, +\pi)$ is the restricted phase error. The loop equation for the restricted phase

error process $\{\Psi(k)\}$ is

$$\Psi(k) = (1 - G_1)\Psi(k-1) - G_1 n_\theta(k-1) + a_1. \quad (26)$$

The pdf of $\Psi(k)$ can be obtained by solving the corresponding C-K equation numerically in the interval $(-\pi, +\pi)$ as

$$p_k(\Psi \mid \Psi_0) = \int_{-\pi}^{\pi} r(\Psi \mid z) p_{k-1}(z \mid \Psi_0)\, dz \quad (27)$$

where $\Psi_0 \triangleq \Psi(0)$. As $k \to \infty$, the steady-state pdf of the phase error Ψ exists and is unique, independent of initial phase error Ψ_0. Therefore, $\lim_{k\to\infty} p_k(\Psi \mid \Psi_0) \triangleq p(\Psi)$ could be obtained by solving the following equation

$$p(\Psi) = \int_{-\pi}^{+\pi} r(\Psi \mid z) p(z)\, dz \quad (28)$$

numerically. From (26), the steady-state mean of the phase error $\Psi(k)$ as $k \to \infty$ in the presence of noise is

$$E[\Psi_{ss}] = (1 - G_1)E[\Psi_{ss}] - G_1 E\left[\lim_{k\to\infty} n_\theta(k)\right] + a_1. \quad (29)$$

In the case of relatively high SNR of the input signal, $E[\Psi_{ss}]$ can be approximated by a_1/G_1 with $E[n_\theta(k)]$ being very small compared with other terms in the equation. It is necessary here that $|a_1/G_1| < \pi$ since $E[\Psi_{ss}]$ must lie in the interval $(-\pi, +\pi)$. By squaring (26), taking the expectation of both sides and letting $k \to \infty$, it follows

$$\mathrm{var}[\Psi_{ss}] = E[\Psi_{ss}^2] - \{E[\Psi_{ss}]\}^2 = \frac{G_1}{2 - G_1}\mathrm{var}[n_\theta]. \quad (30)$$

We notice that $\mathrm{var}[\Psi_{ss}]$ decreases as G_1 decreases. Also, with the increase of input signal SNR value, $\mathrm{var}[n_\theta]$ decreases, so does $\mathrm{var}[\Psi_{ss}]$.

The Second-Order Loop: As in the case of the first-order loop, performance analysis is focused on the behavior of the restricted phase error process $\{\Psi(k)\}$ in the steady-state. With the quadratic input phase, the loop equation in the presence of noise is

$$\begin{aligned}\Psi(k) - 2\Psi(k-1) + \Psi(k-2) &= 2a_2 - G_1 r[\Psi(k-1) + n_\theta(k-1)] \\ &\quad + G_1[\Psi(k-2) + n_\theta(k-2)]. \end{aligned} \quad (31)$$

This equation does not assure that the phase error process $\{\Psi(k)\}$ is a Markov process, therefore we may rewrite it in a set of first-order stochastic difference equations as

$$\begin{aligned} x_1(k) &= x_2(k-1) \\ x_2(k) &= (G_1 - 1)x_1(k-1) \\ &\quad + (2 - rG_1)x_2(k-1) + G_1 n_\theta(k-1) \end{aligned} \quad (32)$$

and the corresponding output difference equation is

$$\Psi(k) = x_1(k) - r x_2(k) + \frac{2a_2}{G_2}. \quad (33)$$

The vector process $\{x_1(k), x_2(k)\}$ can be regarded as a first-order, two-dimensional Markov process, which satisfies the two-dimensional C-K equation. It can be derived [14] that the steady-state joint pdf of x_1 and x_2 is the only solution of the following steady-state equation

$$p(x_1, x_2) = \int_{-\pi}^{\pi} \tilde{r}(x_2 \mid z_1, x_1) p(z_1, x_1)\, dz_1 \quad (34)$$

where

$$\tilde{r}(x_2 \mid z_1, x_1) = \sum_{n=-\infty}^{\infty} \tilde{q}_k(x_2 + 2n\pi \mid z_1, x_1) \quad (35)$$

and

$$\tilde{q}_k(x_2 \mid z_1, x_1) = \begin{cases} \dfrac{1}{G_1}\dfrac{\exp(-\alpha)}{2\pi} + \dfrac{1}{G_1}\dfrac{\sqrt{\alpha}}{\sqrt{\pi}}\cos\left(\dfrac{x_2 - x_{2p}}{G_1}\right) \\ \quad \times \exp\left[-\alpha \sin^2\left(\dfrac{x_2 - x_{2p}}{G_1}\right)\right] \\ \quad \times \left\{\dfrac{1}{2} + \mathrm{erf}\left[\sqrt{2\alpha}\cos\left(\dfrac{x_2 - x_{2p}}{G_1}\right)\right]\right\} \\ \quad \text{if} \quad x_2 \in (-z_1 + 2x_1 - G_1\pi, -z_1 + 2x_1 + G_1\pi) \\ 0, \quad \text{if} \quad x_2 \notin (-z_1 + 2x_1 - G_1\pi, -z_1 + 2x_1 + G_1\pi) \end{cases} \quad (36)$$

with $x_{2p} = (G_1 - 1)z_1 + (2 - rG_1)x_1$. From probability theory [15] and from (33)–(34), the steady-state pdf of the phase tracking error $\Psi(k)$ is

$$p(\Psi) = \int_{-\pi}^{\pi}\left[\int_{-\pi}^{\pi} \tilde{r}\left(x_2 \mid z_1, \Psi + rx_2 - \frac{2a_2}{G_2}\right) \cdot p\left(z_1, \Psi + rx_2 - \frac{2a_2}{G_2}\right) dz_1\right] dx_2 \quad (37)$$

which can be calculated numerically.

The steady-state mean of the phase tracking error is obtained by taking the expectations of both sides of (32)–(33) and letting $k \to \infty$,

$$\begin{aligned} E[x_{1ss}] &= E[x_{2ss}] \\ E[x_{2ss}] &= (G_1 - 1)E[x_{1ss}] + (2 - rG_1)E[x_{2ss}] \\ &\quad + G_1 \lim_{k\to\infty} E[n_\theta(k)] \\ E[\Psi_{ss}] &= E[x_{1ss}] - rE[x_{2ss}] + \frac{2a_2}{G_2}. \end{aligned} \quad (38)$$

With $E[n_\theta(k)]$ being very small compared with other terms, $E[\Psi_{ss}] = 2a_2/G_2$. Squaring both sides of (32)–(33) and taking the expectation of each term, in steady-state, it follows that the variance of the phase

tracking error due to input noise is

$$\text{var}[\Psi_{ss}] = E[\Psi_{ss}^2] - \{E[\Psi_{ss}]\}^2 = \frac{2(r-1)+G_1(r+1)}{4-G_1(r+1)}\text{var}[n_\theta] \quad (39)$$

where $r > 1$ and $0 < G_1 < 4/(r+1)$ since $\text{var}[\Psi_{ss}] \geq 0$. We observe that $|E[\Psi_{ss}]|$ decreases as the system dynamic parameter $|a_2|$ decreases and/or loop gain G_2 increases. Also, $\text{var}[\Psi_{ss}]$ decreases as G_1 and/or r decreases, and as the SNR value of input signal increases which reduces $\text{var}[n_\theta]$.

The Third-Order Loop: With the cubic input phase, from (5), the third-order loop difference equation for the restricted phase tracking error process $\{\Psi(k)\}$ is

$$\begin{aligned}\Psi(k) - 3\Psi(k-1) + 3\Psi(k-2) - \Psi(k-3) &= 6a_3 - pG_1[\Psi(k-1) + n_\theta(k-1)] \\ &\quad + (1+r)G_1[\Psi(k-2) - n_\theta(k-2)] \\ &\quad - G_1[\Psi(k-3) + n_\theta(k-3)]. \end{aligned} \quad (40)$$

The loop equation can be represented in the form of a set of first-order, three-dimensional state equations as

$$\begin{aligned} x_1(k) &= x_2(k-1) \\ x_2(k) &= x_3(k-1) \\ x_3(k) &= (1-G_1)x_1(k-1) \\ &\quad + [(1+r)G_1 - 3]x_2(k-1) \\ &\quad + (3 - pG_1)x_3(k-1) + G_1 n_\theta(k-1) \end{aligned} \quad (41)$$

and the corresponding output equation is

$$\Psi(k) = -x_1(k) + (1+r)x_2(k) - px_3(k) + 6a_3/G_3. \quad (42)$$

The steady-state joint pdf $p(x_1, x_2, x_3)$ exists and is unique, independent of the initial state of vector $\{x_1(0), x_2(0), x_3(0)\}$. It can be obtained by numerically solving the equation [13]

$$p(x_1, x_2, x_3) = \int_{-\pi}^{\pi} \bar{r}(x_3 \mid z_1, x_1, x_2) \cdot p(z_1, x_1, x_2)\, dz_1 \quad (43)$$

where

$$\bar{r}_{k-1}(x_3 \mid z_1, x_1, x_2) \triangleq \sum_{l=-\infty}^{\infty} \tilde{q}_{k-1}(x_3 + 2l\pi \mid z_1, x_1, x_2) \quad (44)$$

and

$$\tilde{q}_{k-1}(x_3 \mid z_1, x_1, x_2) = \begin{cases} \dfrac{1}{G_1}\dfrac{\exp(-\alpha)}{2\pi} + \dfrac{1}{G_1}\dfrac{\sqrt{\alpha}}{\sqrt{\pi}}\cos\left(\dfrac{x_3 - x_{3p}}{G_1}\right) \\ \quad \times \exp\left[-\alpha \sin^2\left(\dfrac{x_3 - x_{3p}}{G_1}\right)\right] \\ \quad \times \left\{\dfrac{1}{2} + \text{erf}\left[\sqrt{2\alpha}\cos\left(\dfrac{x_3 - x_{3p}}{G_1}\right)\right]\right\} \\ \quad \text{if} \quad x_3 \in (-z_1 - 3z_2 + 3z_3 - G_1\pi, z_1 - 3z_2 + 3z_3 + G_1\pi) \\ 0, \quad \text{if} \quad x_3 \notin (-z_1 - 3z_2 + 3z_3 - G_1\pi, z_1 - 3z_2 + 3z_3 + G_1\pi). \end{cases} \quad (45)$$

Based on (42) and the joint pdf of the state variables x_1, x_2, and x_3 obtained from (43), the steady-state pdf of the phase tracking error Ψ can be calculated from the following equation

$$p(\Psi) = \int_{-\pi}^{\pi}\int_{-\pi}^{\pi} \frac{1}{p} p\left(y_1, y_2, \frac{-y_1 + (1+r)y_2 - \Psi}{p}\right) dy_1\, dy_2. \quad (46)$$

Taking the expectations of both sides of (40), with $E[n_\theta(k)] \approx 0$, the steady-state mean of the phase error is obtained as $E[\Psi_{ss}] \approx 6a_3/G_3$. From (40), the variance of the phase error is

$$\text{var}[\Psi_{ss}] = E[\Psi_{ss}^2] - \{E[\Psi_{ss}]\}^2 = \frac{[(r^2+4p^2-8rp) + (2p+p^2+2rp+rp^2-2r-3r^2-r^3)G_1]G_1 E[n_\theta^2]}{16(r-p) + (-12r+12p-10r^2+2p^2+8rp)G_1 + (1+r)(2r+r^2-2p-p^2)G_1^2}. \quad (47)$$

Summarizing the above analysis, it is observed that the steady-state pdf of the loops depends on the loop gain parameter(s). With smaller values of the gain parameters, the steady-state phase tracking error due to input noise decreases, which can also be seen from the variances of the phase error (i.e., (30), (39), and (47)). However, lower loop gain parameters degrade the dynamic tracking capability of the loops, as discussed in Section III. Generally, the phase error comes from both input phase dynamics and noise, and the selection of optimal loop gain parameter(s) depends on which, the receiver dynamics or the input noise, is the dominant source of the phase error.

V. ACQUISITION PROBABILITY AND MEAN TIME TO THE FIRST CYCLE-SLIPPING

In the following, we consider statistics related to instantaneous phase error, including carrier phase acquisition at the kth step and mean time to the first cycle-slipping.

Carrier Phase Acquisition Performance: The input carrier phase acquisition is the process of reducing the arbitrary initial phase error until it lies in the domain $(-\varepsilon, +\varepsilon)$, where ε is a small positive number, e.g., $\varepsilon \in (0.05\pi, 0.10\pi)$. The acquisition is reached at the kth step if, for every $i \geq k$, $|\Psi(i)| < \varepsilon$. Here, it is assumed that the order of the loop is high enough to cope with the system dynamics so that the steady-state phase error due to system dynamics is $\Psi_{ss} \approx 0$. A valuable statistic is the number of expected steps required for the phase error to reach the interval $(-\varepsilon, +\varepsilon)$ for the first time given that it was initially at $\Psi(0)$, which can be modeled as a first passage time problem [16]. To solve this problem, absorbing boundaries $\Psi(k) = \pm\varepsilon$ are set in the pdf of the phase error $\Psi(k)$ and the acquisition process is stopped (absorbed) once the phase error $\Psi(k)$ has fallen within the interval $(-\varepsilon, +\varepsilon)$. For a first-order loop, the pdf of the phase error in the acquisition process is

$$p_k(\Psi \mid \Psi_0) = \begin{cases} 0, & -\varepsilon \leq \Psi \leq +\varepsilon \\ \displaystyle\int_{-\pi}^{\pi} q_{k-1}(\Psi \mid z) \cdot p_{k-1}(z \mid \Psi_0)\, dz, & -\pi \leq \Psi < -\varepsilon, \quad \varepsilon < \Psi \leq \pi \end{cases} \tag{48}$$

where $q_{k-1}(\cdot \mid \cdot)$ is defined in (24). When $k = 0$,

$$p_0(\Psi \mid \Psi_0) = \delta(\Psi_0), \qquad p_0(\Psi) = \int_{-\pi}^{\pi} p_0(\Psi \mid \Psi_0) \cdot p(\Psi_0)\, d\Psi_0 = p(\Psi_0) \tag{49}$$

when $k \neq 0$,

$$p_k(\Psi) = \begin{cases} 0, & -\varepsilon \leq \Psi \leq +\varepsilon \\ \displaystyle\int_{-\pi}^{\pi} q_{k-1}(\Psi \mid z) \cdot p_{k-1}(z)\, dz, & -\pi \leq \Psi < -\varepsilon, \quad +\varepsilon < \Psi \leq \pi. \end{cases} \tag{50}$$

In the acquisition process, the pdf of the phase error is related to the transient response of the initial phase coarse synchronization, not the steady-state pdf discussed earlier. As a result, the transient pdf in the acquisition stage is not independent of initial phase error. Without a priori information, the initial phase error $\Psi(0)$ is assumed to be uniformly distributed over $(-\pi, +\pi)$. The absorption probability at the kth step is

$$p_{acq}(k) = \int_{-\pi}^{\pi} [p_{k-1}(\Psi) - p_k(\Psi)]\, d\Psi. \tag{51}$$

If the initial phase error $\Psi(0)$ is in the region $[-\varepsilon, +\varepsilon]$, then no phase acquisition is needed and the DPLL goes immediately to phase fine tracking. The acquisition process is thus necessary only when $|\Psi(0)| > \varepsilon$. Therefore, with an initial phase uniformly distributed over $[-\pi, +\pi]$, the probability of initial acquisition is $p_{acq}(0) = \varepsilon/\pi$. From (49)–(51), the acquisition probability $p_{acq}(k)$ can be calculated numerically.

Mean Time to First Cycle-Slipping: In the fine synchronization of the phase tracking, due to input phase dynamics and/or input noise, synchronization failures may occur, which means that the unrestricted phase tracking error $\psi(k)$ changes from the initial lock point $\psi(0)$ to outside of the interval $[\psi(0) - 2\pi, \psi(0) + 2\pi]$, that is, $|\Delta\psi|/2\pi > 1$. This phenomenon is called cycle-slipping. Cycle-slipping characterizes the dynamic phase error in fine tracking process. It can be described by the mean number of steps after which the first cycle-slipping occurs. Cycle-slipping due to input noise is studied here. We consider $\psi(0) = 0$, which is the case when both the carrier phase and the frequency of the local NCO is locked to those of the input signal. For a first-order loop, the phase error process $\{\psi(k)\}$ is described by (22) with $a_1 = 0$. To calculate the probability of the first cycle-slipping, the absorbing boundaries of the phase error pdf are set at $\psi = \pm 2\pi$, i.e., $p_k(\psi) = 0$ if $|\psi| > 2\pi$. Once $|\psi| = 2\pi$ is reached, the system is assumed to stop functioning. The corresponding C-K equation is

$$p_k(\psi \mid \psi_0 = 0) = \int_{-2\pi}^{2\pi} q(\psi \mid u) \cdot p_{k-1}(u \mid \psi_0 = 0)\, du \tag{52}$$

where $q_{k-1}(\psi \mid u)$ is defined in (24) with $a_1 = 0$. The probability of the first cycle slip occurring at the kth step, $p_{cs}(k)$, can be obtained by differencing the probabilities of cycle slip occurring at step numbers larger than $k-1$ and larger than k, respectively, i.e.,

$$p_{cs}(k) = \int_{-2\pi}^{2\pi} [p_{k-1}(\psi \mid \psi_0 = 0) - p_k(\psi \mid \psi_0 = 0)]\, d\psi. \tag{53}$$

The mean number of steps to the first cycle-slipping is thus

$$\overline{K} \triangleq \sum_{k=1}^{\infty} k\, p_{cs}(k) = 1 + \int_{-2\pi}^{2\pi} \sum_{k=1}^{\infty} p_k(\psi \mid \psi_0 = 0)\, d\psi \tag{54}$$

where the constant 1 comes from the fact that $p_0(\psi \mid \psi_0) = \delta(0)$. Define

$$P(\psi \mid \psi_0 = 0) = \sum_{k=1}^{\infty} p_k(\psi \mid \psi_0 = 0) \tag{55}$$

then from (52), it follows

$$P(\psi \mid \psi_0 = 0) = \sum_{k=0}^{\infty} p_{k+1}(\psi \mid \psi_0)$$

$$= q(\psi \mid 0) + \int_{-2\pi}^{2\pi} q(\psi \mid u) \cdot P(u \mid \psi_0 = 0)\, du. \quad (56)$$

By computing $P(\psi \mid \psi_0 = 0)$ numerically, the mean steps $\overline{K}$ to the first cycle-slipping can be obtained numerically from the following equation

$$\overline{K} = 1 + \int_{-2\pi}^{2\pi} P(\psi \mid \psi_0 = 0)\, d\psi \quad (57)$$

and the mean time of the first cycle-slipping is $\overline{K}NT_s$. For a second-order loop, the mean step number of the first cycle-slipping is (see Appendix)

$$\overline{K} = 1 + \int_{-\pi}^{\pi} dx_2 \int_{-2\pi + rx_2}^{2\pi + rx_2} P(x_1, x_2)\, dx_1 \quad (58)$$

where $P(x_1, x_2)$ can be obtained by

$$P(x_1, x_2) = \int_{-\pi}^{\pi} \tilde{r}(x_2 \mid z_1, x_1) \cdot P(z_1, x_1)\, dz_1 \quad (59)$$

and $\tilde{r}(x_2 \mid z_1, x_1)$ is defined in (35) with $x_{2p} = 2x_1 - z_1 + G_1 \cdot g[z_1 - rx_1]$.

VI. COMPUTER SIMULATION RESULTS

The discrete nature of the digital carrier phase tracking loop makes it possible to simulate the phase synchronization process directly on a computer. Computer simulation results are presented in this section which verify the theoretical DPLL performance analysis of phase tracking errors due to input noise, as discussed in Sections IV–V. In an ideal case with all perturbing forces removed, a GPS satellite orbit is modeled as a Keplerian orbit whose properties are constant with time and can be described by the satellite broadcast ephemeris message parameters and the ephemeris reference time. In the following Monte Carlo simulations, ephemeris data is taken from [17], with satellite "6" in the 347th week of the GPS time and with $f_s = 2.1518$ MHz and $N = 86072$. For a static receiver, the variations of the input signal parameters result only from the satellite dynamics. With the example of the satellite orbit data used, the variations of input signal parameters are very smooth compared with the bandwidth of the DDLL and DPLL, therefore, the errors in the GPS observables result primarily from the input noise. The DPLL operations (including carrier phase acquisition and carrier phase tracking) are simulated after a first-order noncoherent E-L DDLL accurately despreads the PRN code of the input signal (with code phase tracking error less than 0.05 code chip width). After the local NCO tracks the input carrier phase with the phase residual from the DPLL being less than 0.1π, the carrier-aiding technique [2] is used for the code phase tracking to suppress the input noise effect on code phase tracking.

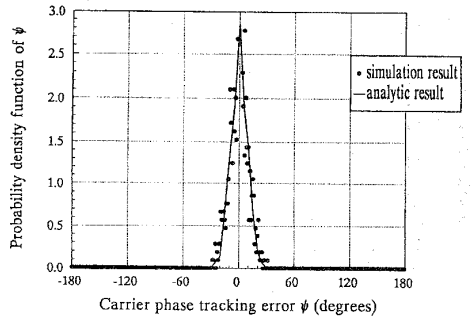

(a)

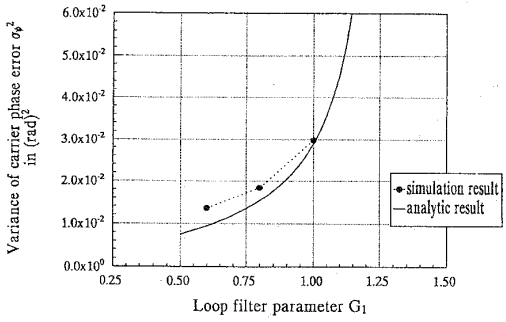

(b)

Fig. 9. Carrier phase error of second-order DPLLs: $C/N_0 = 40$ dB-Hz, $T = 20$ ms. (a) Pdf: $G_1 = 1.0$, $r = 2.0$. (b) Variance: $r = 2.0$.

Carrier Phase Tracking Error: Figs. 9 and 10 show the pdf and variance of phase error of second and third-order DPLLs, respectively, based on simulation data of 30 s coherent tracking of the input code phase and carrier phase of the GPS C/A code signal. For the pdf, the simulation results agree well with the numerical results obtained from (37) and (46). As to the variances, the phase tracking error from the simulation is slightly larger than those from the numerical analysis. The reason is that, in the theoretical analysis of Section IV, no frequency estimation error is taken into account; however, in the simulation, the frequency estimation error (including random estimation noise due to input carrier phase noise) is unavoidable although it is very small (up to a few Hertz) for the static receiver.

Probability of Carrier Phase Acquisition: Fig. 11 shows the phase acquisition probability $p_{acq}(k)$ at

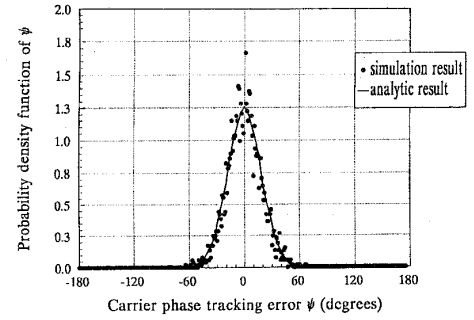

(a)

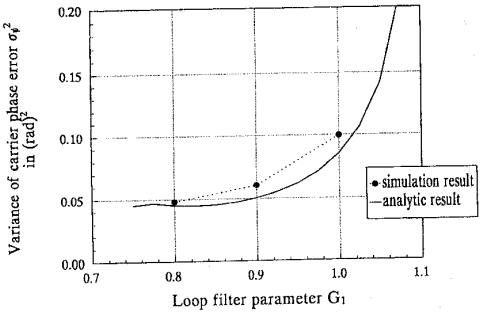

(b)

Fig. 10. Carrier phase error of third-order DPLLs: $C/N_0 = 40$ dB-Hz, $T = 20$ ms. (a) Pdf: $G_1 = 1.0$, $r = 2.0$, $p = 3.0$. (b) Variance: $r = 2.0$, $p = 3.0$.

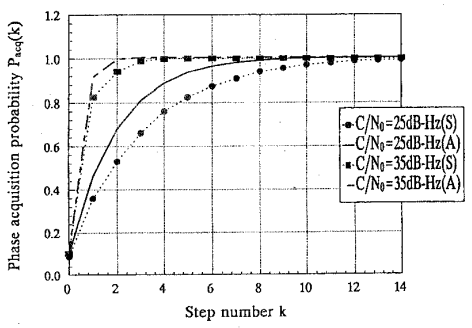

(a)

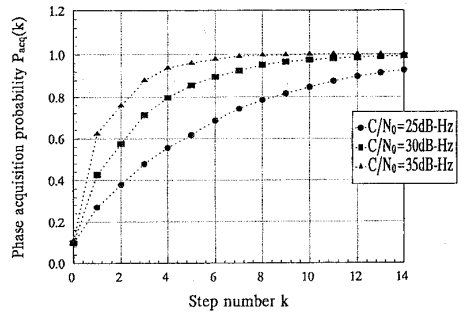

(b)

Fig. 11. Phase acquisition probability. (a) First-order DPLL: $G_1 = 1.0$, $T = 10$ ms. (b) Second-order DPLL: $T = 10$ ms, $G_1 = 1.0$, $r = 2.0$.

the kth step in the carrier phase acquisition process for 1) first-order and 2) second-order DPLLs as a function of input carrier to noise density ratio C/N_0 after noncoherent E-L DDLL despreads the input PRN code. Theoretical $p_{acq}(k)$ is obtained by numerically solving (51) for the first-order loop. Each of the simulation data curve is obtained based on 2000 independent carrier phase acquisition processes. The carrier phase is assumed to be acquired if the residual phase error from the DPLL is in the interval $(-15°, +15°)$. The slight difference between the numerical and simulation results, as shown in Fig. 11(a), is due to a small Doppler frequency shift estimation error existing in the simulation, which is not considered in the theoretical analysis. Generally, after code phase being accurately synchronized, carrier phase acquisition can be obtained over a few steps for a static GPS receiver, provided that the Doppler shift is coarsely acquired. In the receivers, because of system dynamics, second and third-order DPLLs are most often used for carrier tracking. Compared with a second-order loop, a third-order loop can extend the (dynamic) tracking range at the expense of loop stability. Hence, a second-order loop is usually used for phase acquisition. Once the carrier phase is acquired, the loop filter is then switched to a third-order loop mode if necessary. Third-order loop acquisition is therefore not analyzed and simulated here. It is observed that, with a higher C/N_0 value $p_{acq}(k)$ increases; also, a first-order loop has better acquisition performance than a second-order loop. The increase of frequency tracking error, input noise, and input phase dynamics will degrade the acquisition performance.

Probability of First Cycle-Slipping: Simulations on the first cycle slipping in carrier phase tracking are performed for first, second and third-order DPLLs. Fig. 12 shows the analytical result (obtained from (57)) and simulation results of the mean step number of the first cycle slip, $\overline{K}$, for a first-order DPLL. It is observed that the analytical result agrees very well with the simulation result, particularly when C/N_0 of the input signal is equal to or less than 30 dB-Hz. With the C/N_0 value greater than 30 dB-Hz, $\overline{K}$ increases rapidly with the increase of C/N_0, that is, $\overline{K}$ is very sensitive to C/N_0, which leads to the difference between the analytic and simulation results of $\overline{K}$ at a C/N_0 value of 35 dB-Hz. Probabilities of the first cycle slip at the kth step of second and third-order DPLLs are shown in Fig. 13, with each curve based on 3000 independent phase tracking processes. It is observed that the probability decreases dramatically when C/N_0 increases up to a certain value, e.g. 40 dB-Hz. Because higher order loops are more unstable, the probability of cycle-slipping increases as the loop order increases. It should be mentioned that the correlation interval T

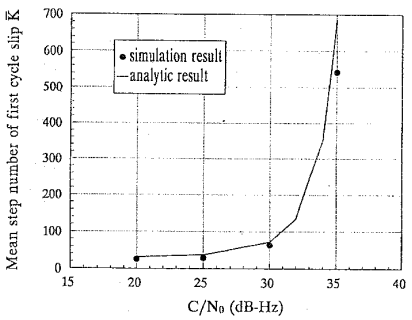

Fig. 12. Mean step number of first cycle-slipping of first-order DPLL. $T = 1$ ms, $G_1 = 0.8$.

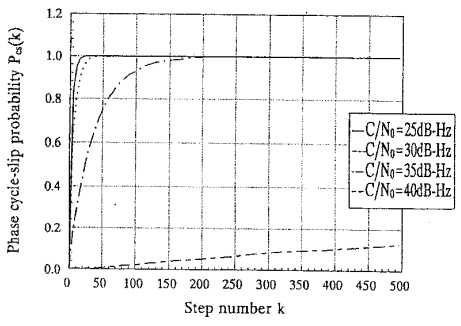

(a)

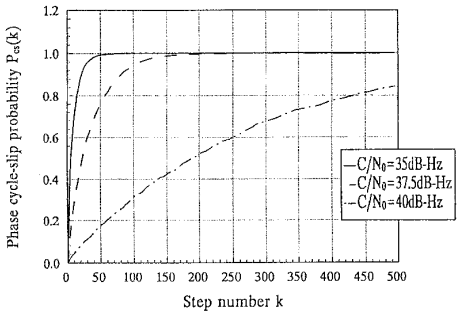

(b)

Fig. 13. Probability of first cycle-slipping of phase tracking. (a) Second-order DPLL: $T = 1$ ms, $G_1 = 0.8$, $r = 2.0$. (b) Third-order DPLL: $T = 1$ ms, $G_1 = 0.8$, $r = 2.0$, $p = 3.0$.

of 1 ms is used in the simulations. Generally T equals 10 ms, 20 ms, or 50 ms, etc. (depending on system dynamics), which means that the SNR value of the DPLL input signal (after the DDLL) are increased correspondingly by 10 dB, 13 dB, or 17 dB, etc. It is expected from Fig. 13 that with $T = 10$ ms, 20 ms, 50 ms, etc., the probability of a carrier phase cycle slip will be very small with low system dynamics and with C/N_0 being greater than 35 dB-Hz. Due to the expected large $\bar{K}$ value for the situation, it is very time consuming to simulate the cycle slip processes on a computer; therefore, the value of $T = 1$ ms is selected for the simulations.

VII. CONCLUSIONS

The performance of the GPS carrier phase observable has been investigated. The observable is obtained by a DPLL. Theoretical analysis has demonstrated that higher order loops with larger gain parameters have better phase tracking performance in the case of highly dynamic input carrier phase, at the expense of the loop stability and the increase of the phase error due to input noise; lower order loops have better phase acquisition performance and less chance of having a cycle slip. Computer simulation results have verified the theoretical analysis. This work provides an important reference in the DPLL design for high accuracy of the GPS phase observable. Although the analysis has been focused on the GPS phase observable, the approach can also be applied to study other carrier phase synchronization process of a spread spectrum system.

APPENDIX. THE MEAN STEP NUMBER OF THE FIRST CYCLE-SLIPPING OF SECOND-ORDER DPLL

For a second-order loop, with a linear input phase, the loop equation is

$$\begin{aligned}\psi(k) - 2\psi(k-1) + \psi(k-2) &= -G_1 r\{g[\psi(k-1)] + n_\theta(k-1)\} \\ &\quad + G_1\{g[\psi(k-2)] + n_\theta(k-2)\} \end{aligned} \tag{60}$$

with the initial phase error $\psi(-1) = \psi(0) = 0$ in fine phase synchronization. In order to apply the C-K equation, we describe the loop by 1st-order two-dimensional state equation as

$$\begin{aligned} x_1(k) &= x_2(k-1) \\ x_2(k) &= 2x_2(k-1) - x_1(k-1) \\ &\quad + G_1 g[x_1(k-1) - r x_2(k-1)] + G_1 n_\theta(k-1) \end{aligned} \tag{61}$$

and the corresponding output equation is

$$\psi(k) = x_1(k) - r x_2(k). \tag{62}$$

The C-K equation for the two-dimensional Markov process $\{x_1(k), x_2(k)\}$ is

$$p_k(x_1, x_2 \mid x_{10}, x_{20}) = \int_{-\pi}^{\pi} \bar{r}(x_2 \mid z_1, x_1) \cdot p_{k-1}(z_1, x_1 \mid x_{10}, x_{20})\, dz_1 \tag{63}$$

where $\bar{r}(x_2 \mid z_1, x_1)$ is defined in (35) with $x_{2p} = 2x_1 - z_1 + G_1 \cdot g[z_1 - r x_1]$. From the initial condition of $\psi(k)$ and (60)–(61), the initial joint pdf of (x_{10}, x_{20}) can be obtained as

$$p(x_{10}, x_{20}) = \delta(x_{10} - r x_{20}) \cdot \tilde{p}(x_{20}). \tag{64}$$

Defining

$$p_k(x_1, x_2) = \int_{-\infty}^{\infty}\int_{-\infty}^{\infty} p_k(x_1, x_2 \mid x_{10}, x_{20}) \cdot p(x_{10}, x_{20})\, dx_{10}\, dx_{20} \tag{65}$$

and

$$\tilde{p}(x_{20}) = \begin{cases} \dfrac{(1-r)^2}{G_1}\dfrac{\exp(-\alpha)}{2\pi} + \dfrac{(1-r)^2}{G_1}\dfrac{\sqrt{\alpha}}{\sqrt{\pi}}\cos\left[\dfrac{(1-r)^2 x_{20}}{G_1}\right] \\ \quad \times \exp\left\{-\alpha \sin^2\left[\dfrac{(1-r)^2 x_{20}}{G_1}\right]\right\} \\ \quad \times \left\{\dfrac{1}{2} + \operatorname{erf}\left(\sqrt{2\alpha}\cos\left[\dfrac{(1-r)^2 x_{20}}{G_1}\right]\right)\right\} \\ \qquad \text{if} \quad X_{20} \in \left(-\dfrac{(1-r)^2\pi}{G_1}, +\dfrac{(1-r)^2\pi}{G_1}\right) \\ 0, \quad \text{if} \quad X_{20} \notin \left(-\dfrac{(1-r)^2\pi}{G_1}, +\dfrac{(1-r)^2\pi}{G_1}\right) \end{cases} \tag{66}$$

$$P(x_1, x_2) = \sum_{k=1}^{\infty} p_k(x_1, x_2), \qquad P(\psi) = \sum_{k=1}^{\infty} p_k(\psi \mid \psi_0 = 0) \tag{67}$$

then from (63), (59) follows and

$$P(\psi) = \int_{-\pi}^{\pi} P(\psi + r x_2, x_2)\, dx_2. \tag{68}$$

From the analysis similar to that of the first-order loop cycle-slipping performance, the mean step number of the first cycle-slipping for a second-order loop can be derived as (58).

REFERENCES

[1] Getting, I. A. (1993)
The Global Position System.
IEEE Spectrum, **30**, 12 (Dec. 1993), 36–47.

[2] Zhuang, W., and Tranquilla, J. (1993)
Digital baseband processor for the GPS receiver—modeling and simulation.
IEEE Transactions on Aerospace and Electronics Systems, **29**, 4 (Oct. 1993), 1343–1349.

[3] Zhuang, W., and Tranquilla, J. (1994)
Modeling and analysis for the GPS pseudorange observable.
IEEE Transactions on Aerospace and Electronics Systems, **31**, 2 (April 1995), 739–751.

[4] Remondi, B. W. (1984)
Using the Global Positioning System (GPS) phase observable for relative geodesy: Modeling, processing, and results.
Ph.D. dissertation, Center for Space Research, University of Texas at Austin, May 1984.

[5] Lindsey, W. C., and Chie, C. M. (1981)
A survey of digital phase-locked loops.
Proceedings of the IEEE, **69**, 4 (Apr. 1981), 140–431.

[6] Weinberg, A., and Liu, B. (1974)
Discrete time analysis of non-uniform sampling first- and second-order digital phase-locked loops.
IEEE Transactions on Communications, **COM-22**, 2 (Feb. 1974), 123–137.

[7] Chie, C. M. (1977)
Analysis of digital phase-locked loops.
Ph.D. dissertation, Department of Electrical Engineering, University of Southern California, Los Angeles, Jan. 1977.

[8] Lee, J. C., and Un, C. K. (1982)
Performance analysis of digital tanlock loop.
IEEE Transactions on Communications, **COM-30**, 10 (Oct. 1982), 2398–2411.

[9] Cahn, C. R., and Leimer, D. K. (1980)
Digital phase sampling for microcomputer implementation of carrier acquisition and coherent tracking.
IEEE Transactions on Communications, **COM-28**, 8 (Aug. 1980), 1190–1196.

[10] Greco, J., Garodnick, J., and Schilling, D. L. (1974)
Response of an all digital phase-locked loop.
IEEE Transactions on Communications, **COM-22**, 6 (June 1974), 751–764.

[11] Robinson, L. M. (1962)
TANLOCK: A phase-lock loop of extended tracking capability.
Proceedings of IRE Military Electronics, Los Angeles, CA, Feb. 1962, 396–421.

[12] Balodis, M. (1964)
Laboratory comparison of TANLOCK and phaselock receivers.
Conference Records, National Telemetry Conference, 1964, paper 5-4.

[13] Zhuang, W. (1992)
Composite GPS receiver modeling, simulations and applications.
Ph.D. dissertation, Department of Electrical Engineering, University of New Brunswick, Fredericton, Canada, Oct. 1992.

[14] Hasan, P., and Brunk, M. (1986)
Exact calculation of phase-locked loop lock-in frequency.
Electronics Letters, **22**, 25 (Dec. 1986).

[15] Doob, J. L. (1953)
Stochastic Processes.
New York: Wiley, 1953.

[16] Viterbi, A. J. (1966)
Principles of Coherence Communication.
New York: McGraw-Hill, 1966.

[17] Kleusberg, A., Georgiadou, Y., Van Den Heuvel, F., and Heroux, P. (1989)
Single and dual frequency GPS data preprocessing with DIPOP 2.1.
Technical memorandum TM-21, Department of Surveying Engineering, University of New Brunswick, Fredericton, Nov. 1989.

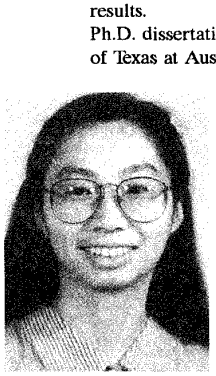

Weihua Zhuang (M'94) received the B.Sc. (1982) and M.Sc. (1985) degrees from Dalian Marine University, China, and the Ph.D. degree (1993) from the University of New Brunswick, Canada, all in electrical engineering.

From January 1992 to September 1993, she was a Post Doctoral Fellow first at the University of Ottawa and then at Telecommunications Research Labs (TRLabs, Edmonton). Since October 1993, she has been with the Department of Electrical and Computer Engineering, University of Waterloo, where she is an Assistant Professor. Her research interests include radio positioning and wireless digital communications.